https://doi.org/10.1016/j.jmst.2019.10.034

Research Article

Enhancing strength and plasticity by pre-introduced indent-notches in $Zr_{36}Cu_{64}$ metallic glass: A molecular dynamics simulation study

Shidong Feng [a,b,*], Lin Li [c], K.C. Chan [b,*], Lei Zhao [b], Limin Wang [a], Riping Liu [a]

[a] *State Key Laboratory of Metastable Materials Science and Technology, Yanshan University, Qinhuangdao 066004, China*

[b] *Advanced Manufacturing Technology Research Centre, Department of Industrial and Systems Engineering, The Hong Kong Polytechnic University, 999077, Hong Kong.*

[c] *Department of Metallurgical and Materials Engineering, The University of Alabama, Tuscaloosa, AL 35487, USA*

* Corresponding author.

E-mail address: shidongfeng@ysu.edu.cn (S.D. Feng);

kc.chan@polyu.edu.hk (K.C. Chan).

Abstract

The deformation behavior in $Zr_{36}Cu_{64}$ metallic glasses with pre-introduced indent-notches has been studied by molecular dynamics simulation at the atomic scale. The indent-notches can trigger the formation of densely-packed clusters composed of solid-like atoms in the indent-notch affected zone. These densely-packed clusters are highly resistant to the nucleation of shear bands. Hence, there is more tendency for the shear bands to nucleate outside the indent-notch affected zone, which enlarges the deformation region and enhances both the strengthening effect and the plastic deformation ability. For indent-notched MGs, when determining the initial yielding level, there is a competition process occurring between the densely-packed clusters

leading to the shear band formation outside the indent-notch affected zone and the stress-concentration localizing deformation around the notch roots. When the indent-notch depth is small, the stress-concentration around the notch root plays a dominant role, leading to the shear bands initiating from the notch root, reminiscence of the cut-notches. As the indent-notch depth increases, there are many densely-packed clusters with high resistance to deformation in the indent-notch affected zone, leading to the shear band formation from the interface between the indent-notch affected zone and the matrix. Current research findings provide a feasible means for improving the strength and the plasticity of metallic glasses at room temperature.

Keywords: metallic glass; notch; shear band; microstructure; molecular dynamics simulation

1. Introduction

Brittle fracture of metallic glasses (MGs) at room temperature is a stumbling block as structural materials [1, 2]. Introducing notches is a very effective way to prevent the brittle fracture of MGs [3-7]. The effects of notch shape, size and orientation on the deformation of MGs have been extensively studied [8-12], and play a key role in understanding the plasticity of notched MGs. However, contradictory notch effects have been observed due to differences in the location and geometry of particular notches. The weakening, strengthening and even insignificant effects of notches on strength have been observed [13-16]. For example, Gu et al. found that the introduction of notches can enable the failure strength to be reduced by 40% and change the fracture mode of MGs from shear band to cavitation [17]. Sha et al. used molecular dynamics (MD) simulation to find that symmetrical double-edge notches can cause strengthening by constraining the growth of the plastic zone for nanoscale MGs [18]. Cui et al. found that notches can trigger the occurrence of strengthening and structural ordering along

with the recovery of Voronoi volume and Cu-centered full-icosahedra during plastic deformation in $Cu_{64}Zr_{36}$ MGs [19]. Qu et al. found that notches can improve the plasticity of MGs, but are insensitive to tensile strength [20]. Yang et al. concluded that different inter-void ligament distance can lead to different degrees of strengthening effects for notched MGs [21]. The key factors affecting the strength of notched MGs are complex and diverse, but it is certain that these notches, which are formed by cutting part of the MGs, destroy the integrity of MGs themselves.

Here, we propose a new way of introducing notches without sacrificing the integrity of MGs. Indentation is usually used to study the mechanical properties of MGs [22, 23]. During the indentation of MGs, the deformation units are activated firstly in the soft zones near the indenter, and then mature shear bands are formed with further loading [24]. Due to the multi-axial stress state beneath the indenter, multiple shear bands form in a semicircular and radial fashion, allowing sustainable plastic flow in MGs [25]. For the indent-notched MGs, there are numerous fundamental questions to be asked. (1) How would the indent-notches affect the deformation behavior of MGs, i.e., strengthening or weakening, enhancement or embrittlement? (2) How are such effects compared with cut-notches? (3) How would this deformation behavior be related with the atomic-level strain and the amorphous structure induced by the indent-notch?

In this study, using $Zr_{36}Cu_{64}$ MGs as a model system, we employ MD simulations to perform a systematic study on the effect of indent-notches in order to understand the relationship between indent-notches and deformation behavior at the atomic level. The paper is organized as follows: in Section 2, the methods and details of MD simulations are described. Section 3 presents the results of the enhanced strengthening effect and the plastic deformation ability induced by indent-notches. Section 4 discusses the underlying mechanisms. Section 5 contains the conclusions.

2. Materials and Methods

MD simulation based on the combination of the large-scale atomic/molecular massively parallel simulator (LAMMPS) and the empirical embedded atom method (EAM) potential was performed [26, 27]. The initial model $Zr_{36}Cu_{64}$ consisted of a square box of 5.8 nm with a random distribution of 3,600 Zr atoms and 6,400 Cu atoms. An *NPT* (constant number, constant pressure, and constant temperature) ensemble with a Nosé-Hoover thermostat and barostat was adopted [28, 29]. It was equilibrated at 2000 K and was quenched to 50 K at a cooling rate of 1.0×10^{12} K/s and hydrostatic pressure 0 Pa under periodic boundary conditions (PBCs). By replicating 7, 1 and 14 times in the *X*, *Y*, and *Z*-directions of the small MG model, a large-scale model containing 980,000 atoms (38.5 nm × 5.5 nm × 77 nm) was obtained. To eliminate the interface effect caused by replication, the large model was relaxed at 800 K for 1 ns and was cooled to 50 K at 1.0×10^{12} K/s under PBCs.

The symmetrical surface notches were formed by cutting and indenting respectively, as shown in **Figure 1**. The cutting was achieved by deleting atoms and relaxing the cut-surfaces, the same way as in the literature [18]. Here, we detail the process of achieving an indent-notch, which has a similar geometry to the cut notch. The indention process was started by moving the cylindrical indenter along the *X*-direction into the central location of the left surface at a rate of 3 nm per 100 ps. The radius of the indenter was 3.6 nm and the indentation process was completed after the tip moved laterally 9 nm. Similarly, the indentation process was repeated on the central location of the right surface, and the final configuration is shown in **Figure 1b**. During indentation, the *Z*-direction was set as PBCs. After the indentation, the large model was relaxed at 50 K for 2 ns. Thereafter, uniform tensile deformation was undertaken for the monolithic, cut-notched and indent-notched $Zr_{36}Cu_{64}$ MGs along the *Z*-direction at

a strain rate of 2×10^7 s^{-1} and 50 K, respectively. The *Y*- and *Z*-directions were set as PBCs, while the *X*-direction was set as the free surface. And the free surface was relaxed at 50 K for 1 ns. The selection of low temperature and free surface can promote the formation of shear bands [30].

3. Results

3.1. Stress-strain curves

Figure 2 displays the engineering stress-strain curves of monolithic, cut-notched and indent-notched $Zr_{36}Cu_{64}$ MGs. To facilitate the comparison across different samples, the engineering stress is calculated by normalizing the force with the initial area of the un-notched ligament. Notably, the ultimate tensile strength of the monolithic, cut-notched and indent-notched $Zr_{36}Cu_{64}$ MGs is 2.78 GPa, 4 GPa and 4.25 GPa, respectively. For comparison, the notch sensitivity of the ultimate tensile strength represented by the notch strength ratio (NSR) is adopted. The ratio is defined as the ratio between the ultimate tensile strength of a notched sample to the ultimate tensile strength of an un-notched sample [20]. When the ultimate tensile strength of the notched specimen is larger than that of the un-notched, NSR > 1; Conversely, NSR < 1. Consequently, the NSR of the cut-notched MG is 1.44, while that of the indent-notched MG is 1.53. With similar notch geometry, Sha et al. reported NSR = 1.4 for the cut-notched sample, confirming the reliability of our model [13]. Meanwhile, indent-notches provide an even pronounced strengthening effect, i.e., NSR is larger than that of cut-notches. It's worth noting that the triaxiality generated by the notch mainly influences the mechanical behaviour of MGs [10, 19]. For example, Cui et al. found that by introducing a triaxial stress state by notches, the propagation of the shear band can be suppressed and Voronoi volume recovery occurs in the notch center region during plastic deformation [19]. The size of the model under our study is 38.5 nm × 5.5 nm × 77 nm. The triaxiality is reduced in the thickness direction due to the thin plate of 5.5 nm in thickness. Therefore, if the thickness of the model is increased, the strengthening effect will be more obvious.

To characterize the plasticity of different notched MGs, we compute the notch deformation ratio (NDR), which is defined as the ratio between the strain corresponding to the ultimate tensile strength of a notched sample to that of an un-notched sample. NDR < 1, when the strain corresponding to the ultimate tensile strength of a notched sample is smaller than that of the un-notched. The NDR of the cut-notched MG is about 0.57, while that of the indent-notched MG is about 1. The NDR clearly demonstrates that the indent-notches don't sacrifice deformation strain when enhancing the strengthening effect. It is noteworthy that when the strain reaches 11%, the cut-notched MG is fractured, while the indent-notched MG continues to bear the strain.

For the indent-notched MG, the stress-strain curve shows a relatively stable region after the maximum stress, while for the monolithic and cut-notched MGs, the models experience a sudden drop in stress, corresponding to highly localized strain [30]. The smallest stress drop after the maximum stress for the indent-notched MG corresponds to the best plasticity in the three MGs because the smaller the difference between the ultimate tensile stress and the flow stress, the better the plasticity [31-33]. Therefore, the introduction of the indent-notches can simultaneously improve the strengthening effect and the plastic deformation ability. It is noteworthy that, experimentally, for samples with notches, special measurement standards need to be reached [34]. These standards are difficult to achieve at the atomic scale, which may mislead the determination of Young's modulus due to the localization of actual deformation at the notches [18]. Hence, in our work, we only focus on the effect of notch forming methods on the deformation behaviour of MGs.

3.2. Atomic shear strain and transverse shrinkage

To reveal the deformation mode, the atomic shear strain η^{Mises} is used to measure the local plastic deformation by comparing the atomic positions of the current state to

the undeformed state [35]. To minimize the influence of the structural and thermal fluctuations [16], the atoms with $\eta^{Mises} > 0.3$ are considered being involved in local plastic deformation, as shown in **Figure 3**. The snapshots capture the atomic deformation processes at strains of 7%, 10%, 12% and 15% for the monolithic and the indent-notched MGs, and at strains of 4%, 5%, 7% and 10% for the cut-notched MG.

For the monolithic sample shown in **Figure 3a**, local plastic deformation becomes noticeable at a strain of 7%, when the stress reaches the ultimate tensile strength. On further straining, a penetrating shear band forms at a strain of 10% with 45° angle relative to the loading axis, which leads to the occurrence of catastrophic brittle fracture. For the cut-notched MG in **Figure 3b**, local plastic deformation is initiated from the root of each notch at a strain of 4%; correspondingly the stress reaches the ultimate tensile strength. Pronounced strain localization develops rapidly at a strain of 5%, spreading to the entire region of the ligament between two notches. Thereafter, necking occurs until 10% straining, whereas the sample fails by rupture, a signature of a ductile failure. The observed cut-notch induced brittle to ductile transition of failure is consistent with Sha et al's work [18]. Our notched sample satisfies the geometrical transition condition [18]: $d < (Ly - 2w)/2$, where the notch depth d = 12.6 nm, the width of the model Ly = 38.5 nm and the shear band width w = 5 nm; so that the combination of shear banding and necking is expected.

In the indent-notched MG, very interestingly, the local plastic deformation initiates from the un-notched region far from the notched roots at a strain of 7%, a much more delayed strain when compared to the cut-notched sample at ultimate tensile strength. At a strain of 10%, two intersecting shear bands form, extending the deformation regions outside the ligament and providing sustainable plastic flow. Similar to cut-notches, another two local plastic deformation regions start to develop at

the roots of the indent-notches at 10% strain, expanding to the ligament at 12% strain, and coalescing with the center of the intersecting shear bands at 15% strain. Necking occurs afterwards, eventually leading to the rupture of the sample. It is noted that despite the fact that the cut-notches and indent-notches can both restrain the catrostrophinc shear banding under the multi-axial stress concentration in the vicinity of the notches, the cut-notched MG deforms only within the ligament, fracturing at a strain of 10% accompanied with the stress being almost zero in the stress-strain curves; while the initial shear bands of the indent-notched MG form outside the un-notched ligament, extending the deformation region, and thus improving both the strengthening effect and the plastic deformation ability.

We further provide a quantitative analysis on the deformation evolution across the notch plane. **Figure 4** illustrates the proportion of atoms with η^{Mises} greater than 0.3, and the transverse shrinkage (Ψ) across the notch plane, respectively, as a function of tensile strain. The transverse shrinkage (Ψ)is defined as $\Psi = (W_{1(2)}(t)-W_{1(2)})/W_{1(2)}$ [18]. At the initial stage before 4% strain, the proportion of atoms with η^{Mises} greater than 0.3 and the transverse shrinkage (Ψ) is negligible for all the MGs. For the cut-notched MG, around 4% strain, the proportion of atoms with η^{Mises} greater than 0.3 radically increases; meanwhile the transverse shrinkage (Ψ) has a dramatic increase, corresponding to the stress reaching the ultimate tensile strength. After a strain of 5%, the proportion of atoms involved in plastic deformation saturates. Those atoms, concentrating in the ligament of the sample, contribute to nearly all the further plastic flow, giving rise to a continuous rapid increase of the shrinkage of the notch section. On the other hand, the indent-notched MG barely has atoms involved in plastic deformation before 7% strain. In striking contrast, after yielding, the proportion of atoms involved in plasticity remains increasing, even at 12% strain (vs. 5% for the cut-notched sample), indicating

a large participation of atoms. The wide spread of plastically-deformed atoms dramatically slows down the shrinkage of the notch section, retaining a relatively stable flow after initial yielding. When compared to the un-notched MG, though the cut-notches are able to mitigate the brittle failure, the deformation is nearly localized at the notch ligament, limiting the plasticity. Indent-notches promote more local plastic deformation, simultaneously improving the strengthening and the plastic deformation ability without sacrificing deformation strain.

3.3 Plastic zone size

The cut-notch and the indent-notch share a similar notch geomoetry, but the associated plastic zones are distinct, the size of which is essential to relieve the stress concentration at the notch tip. **Figure 5** shows the plastic zone size (D) for the indent-notched and cut-notched MGs as a function of engineering strain, respectively. The plastic zone size (D) is defined as follows: the area of the region of atoms with large atomic shear strain which is equivalent to the area of a circle ($\pi D^2/4$), where the effective diameter D is used to represent the plastic zone size [16]. This plastic zone size has been used to study the formation of shear bands [36]. As shown in **Figure 5**, the initial plastic zone size D of the indent-notched MG is larger than that of the cut-notched MG due to the pre-deformation induced by indentation. After a strain of 3%, the plastic zone size of the cut-notched MG quickly increases, while that of the indent-notched MG gradually increases after a strain of 6%. Sha et al. found that the stress concentration in CuZr MG samples at the notch tip can be relieved by the growth of localized plastic deformation [16]. This is effective not only for nano-sized MGs, but also for bulk MGs in experimentation [37]. The larger plastic zone size of the indent-notched MG suggests that indent-notches can relieve the stress-concentration around the notch root, improving the strengthening effect and the plastic deformation ability.

4. Discussion

As the two notched samples share a similar geometry, the effects of pre-deformation on the local stress/strain states and glassy structure are essential in understanding their different tensile deformation behavior. **Figure 6a** shows a snapshot of atoms with local shear strain $\eta^{Mises} > 0.3$ at a strain of 7% for the indent-notched MG, and the indent-notched MG at a strain of 0% is regarded as the reference state. The red line in **Figure 6a** shows that local plastic deformation initiates from the middle of the un-notched ligament. **Figure 6b** shows atomic displacement vectors and local shear strain of the indent-notched $Zr_{36}Cu_{64}$ MG at a strain of 0%. Here the indent-notched MG before the indentation is regarded as the reference state. Since indent-notches are formed by indenting, the strain around the indent-notches is introduced as shown in the red region, which is called the indent-notch affected zone (INAZ). By overlapping the positions of the red line in **Figures 6a** and **6b**, it can be found that the shear band forming area during the tensile deformation is the interface between the INAZ and the matrix. Next, we explain why local plastic deformation initiates from the interface in the indent-notched MG, while local plastic deformation initiates from the notch root in the cut -notched MG.

Firstly, the changes in the microstructure caused by the indent-notches before tensile deformation are investigated. The quasi-nearest atom (QNA) is a new parameter that can well characterize the atomic packings of MGs [38-40]. A pair of QNAs is defined as follows: (1) they share a common nearest neighbor; (2) their corresponding Voronoi faces of the Voronoi polyhedron centered by the common nearest neighbor share an edge; (3) they are not the nearest neighbors of each other. The more the number of QNAs (N_Q) around an atom, the looser the atomic packing around the atom, indicating more structural defects. If $N_Q = 0$, the central atom is completely bound and

is not easy to move , so it is called a solid atom [40]. The solid atoms make up skeletal structures in MGs, and their connectivity plays a key role in the deformation of MGs [41-44]. Therefore, the connection of clusters composed of atoms with N_Q = 0 in the INAZ was analyzed. The ratio between the number of clusters with N_Q = 0 and the total atoms in the monolithic (before indentation), cut-notched and indent-notched $Zr_{36}Cu_{64}$ MGs was 25.1%, 23.9% and 33.7%, respectively. The ratio in the indent-notched MG reaches a maximum in the three MGs, which indicates that the indent-notches trigger the formation of more densely-packed clusters. These densely-packed clusters blunt the notch and are not easily triggered by shear stress, providing high resistance to deformation in the INAZ. When the indent-notched MG undergoes uniaxial tensile deformation in the Z direction, the force required to rearrange these densely-packed clusters is larger than that in the undeformed region. Consequently, the formation of shear bands is pushed off from the INAZs. Instead, the shear bands begin to form at the interface area between the INAZ and the matrix. In addition, the atoms in the INAZ underwent displacements in different directions as shown in the yellow arrow in **Figure 6b**, and the pre-strained regions can carry more strain in the subsequent tensile deformation. Therefore, the indent-notches not only affect the initial position of deformation, but also carry more atomic strain in response to the tensile stress, leading to improve the strengthening effect and the deformation ability simultaneously.

The average N_Q for the notched MGs at different strains is also investigated. As shown in **Figure 7**, the average N_Q increases with increasing strain, which suggests that the shearing units gradually increase the degree of defects as the strain increases. The N_Q of the cut-notched MG is larger than that of the indent-notched MG in the whole deformation process. This is because the indent-notches can trigger the formation of densely-packed clusters composed of solid-like atoms in the indent-notch affected zone.

Since densely-packed clusters are highly resistant to the nucleation of shear bands, the N_Q of the indent-notched MG shows relatively stable before 1% strain compared to that of the cut-notched MG. The distribution of densely-packed clusters in the indent-notch affected zones also retains the N_Q steadily rising after 4% strain. The fluctuated N_Q of the cut-notched MG after 4% strain may be related to the Voronoi volume recovery and generation. Cui et al. found that Voronoi volume recovery surpassing its generation occurs in the cut-notched center region during plastic deformation [19].

In order to verify the above, the effect of the indent-notch depth on deformation is investigated as follows. The notch depth can change the fracture mode of notched MGs [18, 21]. For example, through molecular dynamics simulations, Yang et al. found increasing the notch depth can enhance the notch intensification, which changes the deformation mode from shear banding dominated to mixed mode and then to necking governed in $Cu_{50}Zr_{50}$ MGs [21]. **Figure 8** shows the engineering stress-strain curves of the indent-notched MGs with different notch depths *d*. The ultimate tensile strength of the indent-notched MGs with notch depths *d* of 4.4, 8.0 and 12.6 nm is 3.41 GPa, 3.81 GPa and 4.25 GPa, respectively, which suggests that the strengthening effect of indent-notches is more pronounced as the notch depth increases. Sha et al. found that with the cut-notch depth increasing, the notch strengthening becomes more pronounced for nanoscale MGs with symmetric double-edge notches [18]. This indicates that both the cut-notch and the indent-notch can cause more pronounced strengthening by increasing the notch depth. The inserted snapshots in **Figure 8** show the atomic deformation processes at a strain of 12% for the indent-notched MGs with different notch depths.

When the depth is 4.4 nm, a shear band formed from the notch root penetrates the MG, giving rise to the occurrence of brittle fracture. This is because of the stress-concentration around the notch root, which is similar to that in the cut-notched MG.

When the depth is 8.0 nm, two narrow shear bands intersecting each other are formed at the interface area between the matrix and the INAZ. There are two reasons for this: one is the densely-packed clusters leading to the formation of shear bands off the notch root; and the second is the larger plastic zone size of the indent-notched MG relieving the stress-concentration around the notch root, as shown in **Figure 5**. As notch depth increases enough to prohibit the interface area between the matrix and the INAZ (for example, $d \geq 12.6$ nm), the multiple shear bands in the un-notched ligament interact with each other, triggering the occurrence of homogeneous deformation in the un-notched ligament occurs.

The above suggests that for the indent-notched MG in determining the initial yielding, there is a competition process between the densely-packed clusters leading to the shear band formation outside the INAZ and the stress-concentration localizing deformation around the notch roots, as shown in **Figure 9**. When the notch depth is small, there are few densely-packed clusters and the force needed to arrange atoms in the INAZ is small, leading to the stress-concentration around the notch root playing a dominant role. Therefore the local plastic deformation initiates from the notch root, which is similar to that in the cut -notched MG. As the notch depth increases, there are many densely-packed clusters composed of solid atoms and the resistance to deformation is high. Therefore, the force needed to arrange atoms is relatively large and the densely-packed clusters composed of solid atoms in the INAZ play a dominant role compared with the stress-concentration around the notch root. The large force pushes the formation of shear band off the root, leading to local plastic deformation initiating from the interface between the matrix and the INAZ in the indent-notched MG. The indentation successfully blunts the notch, providing hardening and sustainable flow by constraining the shear bands.

5. Conclusions

In summary, MD simulations have been performed to investigate the uniaxial tensile behavior of monolithic, cut-notched and indent-notched $Zr_{36}Cu_{64}$ MGs, focusing on the effects of indent-notches on improving both the strengthening effect and the plastic deformation ability. The NDR clearly demonstrates that the indent-notches do not sacrifice deformation strain when enhancing the strengthening effect, i.e., the NSR is larger than that of cut-notches. The larger plastic zone size of the indent-notched MG due to the pre-deformation induced by indentation can relieve the stress-concentration around the notch root. The indent-notches trigger the formation of more densely-packed clusters with $N_Q = 0$ in the INAZ, leading to the initial shear bands being formed off from the indent-notch affected zone, extending the deformation region. For the indent-notched MGs in determining the initial position of yielding, there is a competition between the densely-packed clusters in the INAZ and the stress-concentration around the notch root in determining the initial position of yielding. When the indent-notch depth is small, there are few densely-packed clusters in the INAZ; the stress-concentration around the notch root plays a dominant role, leading to the shear bands initiating from the notch root, reminiscence of the cut-notches. As the indent-notch depth increases, there are many densely-packed clusters in the INAZ and the resistance to deformation is high, and the densely-packed clusters play a dominant role, leading to the shear band formation from the interface between the INAZ and the matrix. The findings shed light on the advantages of indent-notches in improving the deformation ability of MGs.

Acknowledgments

This work was supported by the National Natural Science Foundation of China under Grant 51801174; and the Program for the Top Young Talents of Higher Learning

Institutions of Hebei under Grant BJ2018021; the Hong Kong Scholars Program under Grant XJ2017049; LL would like to acknowledge the support from the National Science Foundation under grant number CMMI 17-0267.

Additional Information

Declarations of interest: none.

References

[1] J.W. Qiao, *In-situ* dendrite/metallic glass matrix composites: a review, J. Mater. Sci. Technol. 29 (2013) 685-701.

[2] H. Sun, Z. Ning, J. Ren, W. Liang, Y. Huang, J. Sun, X. Xue, G. Wang, Serration and shear avalanches in a ZrCu based bulk metallic glass composite in different loading methods, J. Mater. Sci. Technol. 35 (2019) 2079-2085.

[3] J. Pan, Y.X. Wang, Y. Li, Ductile fracture in notched bulk metallic glasses, Acta Mater. 136 (2017) 126-133.

[4] T. Dutta, A. Chauniyal, I. Singh, R. Narasimhan, P. Thamburaja, U. Ramamurty, Plastic deformation and failure mechanisms in nano-scale notched metallic glass specimens under tensile loading, J. Mech. Phys. Solids 111 (2018) 393-413.

[5] S.F. Guo, K.C. Chan, L. Liu, Notch toughness of Fe-based bulk metallic glass and composites, J. Alloys Compd. 509 (2011) 9441-9446.

[6] J. Qiao, In-situ dendrite/metallic glass matrix composites: a review, J. Mater. Sci. Technol. 29 (2013) 685-701.

[7] J.X. Zhao, R.T. Qu, F.F. Wu, S.X. Li, Z.F. Zhang, Deformation behavior and enhanced plasticity of Ti-based metallic glasses with notches, Philos. Mag. 90 (2010) 3867-3877.

[8] J.X. Zhao, F.F. Wu, R.T. Qu, S.X. Li, Z.F. Zhang, Plastic deformability of metallic glass by artificial macroscopic notches, Acta Mater. 58 (2010) 5420-5432.

[9] J.X. Zhao, Achieving the desirable compressive plasticity by installing notch cluster in metallic glass, Mater. Sci. Eng. A 634 (2015) 134-140.

[10] Z.T. Wang, J. Pan, Y. Li, C.A. Schuh, Densification and strain hardening of a

metallic glass under tension at room temperature, Phys. Rev. Lett. 111 (2013) 135504.

[11] J. Pan, H.F. Zhou, Z.T. Wang, Y. Li, H.J. Gao, Origin of anomalous inverse notch effect in bulk metallic glasses, J. Mech. Phys. Solids 84 (2015) 85-94.

[12] W. Li, H. Bei, Y. Gao, Effects of geometric factors and shear band patterns on notch sensitivity in bulk metallic glasses, Intermetallics 79 (2016) 12-19.

[13] Z.D. Sha, Q.X. Pei, Z.S. Liu, Y.W. Zhang, T.J. Wang, Necking and notch strengthening in metallic glass with symmetric sharp-and-deep notches, Sci. Rep. 5 (2015) 10797.

[14] X. Lei, C. Li, X. Shi, X. Xu, Y. Wei, Notch strengthening or weakening governed by transition of shear failure to normal mode fracture, Sci. Rep. 5 (2015) 10537.

[15] R.T. Qu, P. Zhang, Z.F. Zhang, Notch effect of materials: strengthening or weakening?, J. Mater. Sci. Technol. 30 (2014) 599-608.

[16] Z.D. Sha, Q.X. Pei, V. Sorkin, P.S. Branicio, Y.W. Zhang, H.J. Gao, On the notch sensitivity of CuZr metallic glasses, Appl. Phys. Lett. 103 (2013) 081903.

[17] X.W. Gu, M. Jafary-Zadeh, D.Z. Chen, Z. Wu, Y.-W. Zhang, D.J. Srolovitz, J.R. Greer, Mechanisms of failure in nanoscale metallic glass, Nano Lett. 14 (2014) 5858-5864.

[18] Z.D. Sha, Y. Teng, L.H. Poh, Q.X. Pei, G.C. Xing, H.J. Gao, Notch strengthening in nanoscale metallic glasses, Acta Mater. 169 (2019) 147-154.

[19] W. Cui, J. Pan, D.J. Blackwood, Y. Li, Voronoi volume recovery during plastic deformation in deep-notched metallic glasses, J. Alloys Compd. 776 (2019) 460-468.

[20] R.T. Qu, M. Calin, J. Eckert, Z.F. Zhang, Metallic glasses: Notch-insensitive materials, Scripta Mater. 66 (2012) 733-736.

[21] G.J. Yang, B. Xu, C. Qi, L.T. Kong, J.F. Li, Effect of notch depth on the mechanical behavior of $Cu_{50}Zr_{50}$ metallic glasses revealed by molecular dynamics simulations, Intermetallics 93 (2018) 303-311.

[22] C.A. Schuh, T.G. Nieh, A survey of instrumented indentation studies on metallic glasses, J. Mater. Res. 19 (2004) 46-57.

[23] U. Ramamurty, S. Jana, Y. Kawamura, K. Chattopadhyay, Hardness and plastic deformation in a bulk metallic glass, Acta Mater. 53 (2005) 705-717.

[24] Y.-C. Wang, C.-Y. Wu, J.P. Chu, P.K. Liaw, Indentation behavior of Zr-based metallic-glass films via molecular-dynamics simulations, Metall. Mater. Trans. A 41 (2010) 3010-3017.

[25] S. Xie, E.P. George, Hardness and shear band evolution in bulk metallic glasses after plastic deformation and annealing, Acta Mater. 56 (2008) 5202-5213.

[26] S. Plimpton, Fast parallel algorithms for short-range molecular dynamics, J. Comput. Phys. 117 (1995) 1-19.

[27] Y. Cheng, H. Sheng, E. Ma, Relationship between structure, dynamics, and mechanical properties in metallic glass-forming alloys, Phys. Rev. B 78 (2008) 014207.

[28] W.G. Hoover, Canonical dynamics: equilibrium phase-space distributions, Phys. Rev. A 31 (1985) 1695.

[29] S. Nosé, A unified formulation of the constant temperature molecular dynamics methods, J. Chem. Phys. 81 (1984) 511-519.

[30] A.J. Cao, Y.Q. Cheng, E. Ma, Structural processes that initiate shear localization in metallic glass, Acta Mater. 57 (2009) 5146-5155.

[31] D. Rodney, C. Schuh, Distribution of thermally activated plastic events in a flowing glass, Phys. Rev. Lett. 102 (2009) 235503.

[32] F. Shimizu, S. Ogata, J. Li, Yield point of metallic glass, Acta Mater. 54 (2006) 4293-4298.

[33] S.D. Feng, L. Qi, L.M. Wang, S.P. Pan, M.Z. Ma, X.Y. Zhang, G. Li, R.P. Liu, Atomic structure of shear bands in $Cu_{64}Zr_{36}$ metallic glasses studied by molecular dynamics simulations, Acta Mater. 95 (2015) 236-243.

[34] W. Chen, H. Zhou, Z. Liu, J. Ketkaew, L. Shao, N. Li, P. Gong, W. Samela, H. Gao, J. Schroers, Test sample geometry for fracture toughness measurements of bulk metallic glasses, Acta Mater. 145 (2018) 477-487.

[35] F. Shimizu, S. Ogata, J. Li, Theory of shear banding in metallic glasses and molecular dynamics calculations, Mater. Trans. 48 (2007) 2923-2927.

[36] Z.D. Sha, W.H. Wong, Q.X. Pei, P.S. Branicio, Z.S. Liu, T.J. Wang, T.F. Guo, H.J. Gao, Atomistic origin of size effects in fatigue behavior of metallic glasses, J. Mech. Phys. Solids 104 (2017) 84-95.

[37] R.T. Qu, J.X. Zhao, M. Stoica, J. Eckert, Z.F. Zhang, Macroscopic tensile plasticity of bulk metallic glass through designed artificial defects, Mater. Sci. Eng. A 534 (2012) 365-373.

[38] S.P. Pan, S.D. Feng, J.W. Qiao, W.M. Wang, J.Y. Qin, Correlation between local structure and dynamic heterogeneity in a metallic glass-forming liquid, J. Alloys Compd. 664 (2016) 65-70.

[39] X.F. Niu, S.D. Feng, S.P. Pan, Related structure characters and stability of structural defects in a metallic glass, Materials 11 (2018) 468.

[40] S.D. Feng, K.C. Chan, S.H. Chen, L. Zhao, R.P. Liu, The role of configurational disorder on plastic and dynamic deformation in $Cu_{64}Zr_{36}$ metallic glasses: A molecular dynamics analysis, Sci. Rep. 7 (2017) 40969.

[41] M.Z. Li, C.Z. Wang, S.G. Hao, M.J. Kramer, K.M. Ho, Structural heterogeneity and medium-range order inZr_xCu_{100-x} metallic glasses, Phys. Rev. B 80 (2009) 184201.

[42] S.D. Feng, L. Qi, L.M. Wang, P.F. Yu, S.L. Zhang, M.Z. Ma, X.Y. Zhang, Q. Jing, K.L. Ngai, A.L. Greer, G. Li, R.P. Liu, Structural feature of $Cu_{64}Zr_{36}$ metallic glass on nanoscale: Densely-packed clusters with loosely-packed surroundings, Scripta Mater. 115 (2016) 57-61.

[43] M. Lee, C.-M. Lee, K.-R. Lee, E. Ma, J.-C. Lee, Networked interpenetrating connections of icosahedra: Effects on shear transformations in metallic glass, Acta Mater. 59 (2011) 159-170.

[44] J. Ding, E. Ma, Computational modeling sheds light on structural evolution in metallic glasses and supercooled liquids, npj Comput. Mater. 3 (2017) 9.

Figure captions

Figure 1. The schematic diagram of the notches formed by (a) cutting and (b) indenting respectively. L= 9 nm, R= 3.6 nm, d = 12.6 nm, W= 38.5 nm, W_1= 13.3 nm and W_2= 20.6 nm.

Figure 2. The engineering stress-strain curves of the monolithic, cut-notched and indent-notched $Zr_{36}Cu_{64}$ MGs.

Figure 3. Snapshots of atoms with local shear strain greater than 0.3 at different strains for (a) the monolithic, (b) the cut-notched and (c) the indent-notched MGs.

Figure 4. The proportions of atoms with local shear strain greater than 0.3 (upper panel) and the transverse shrinkage across the notch plane (down panel) for the MGs at different strains.

Figure 5. The plastic zone size (D) for the indent-notched and cut-notched MGs as a function of engineering strain. The inserted snapshot shows the plastic zone for the indent-notched and the cut-notched MGs.

Figure 6. (a) The snapshot of atoms with local shear strain greater than 0.3 at a strain of 7% for the indent-notched MG, and the indent-notched MG at a strain of 0% is regarded as the reference state. (b) Atomic displacement vectors (yellow arrows) and local shear strain of the indent-notched MG at a strain of 0%, and the indent-notched MG before the indentation is regarded as the reference state. The red atomic region is called the indent-notch affected zone (INAZ).

Figure 7. The average number of quasi-nearest atoms (N_Q) for the notched MGs at

different strains.

Figure 8. The engineering stress-strain curves of the indent-notched MGs with the notch depth equaling 4.4, 8.0 and 12.6 nm. The inserts show the snapshots of atoms with local shear strain greater than 0.3 at the strain of 12% for the indent-notched MGs with different notch depth.

Figure 9. Schematic description of the competitive relationship between the densely-packed clusters composed of solid atoms in the NAZ and the stress-concentration around the notch root in the dominant role in the initial position of deformation accompanied by the notch depth.

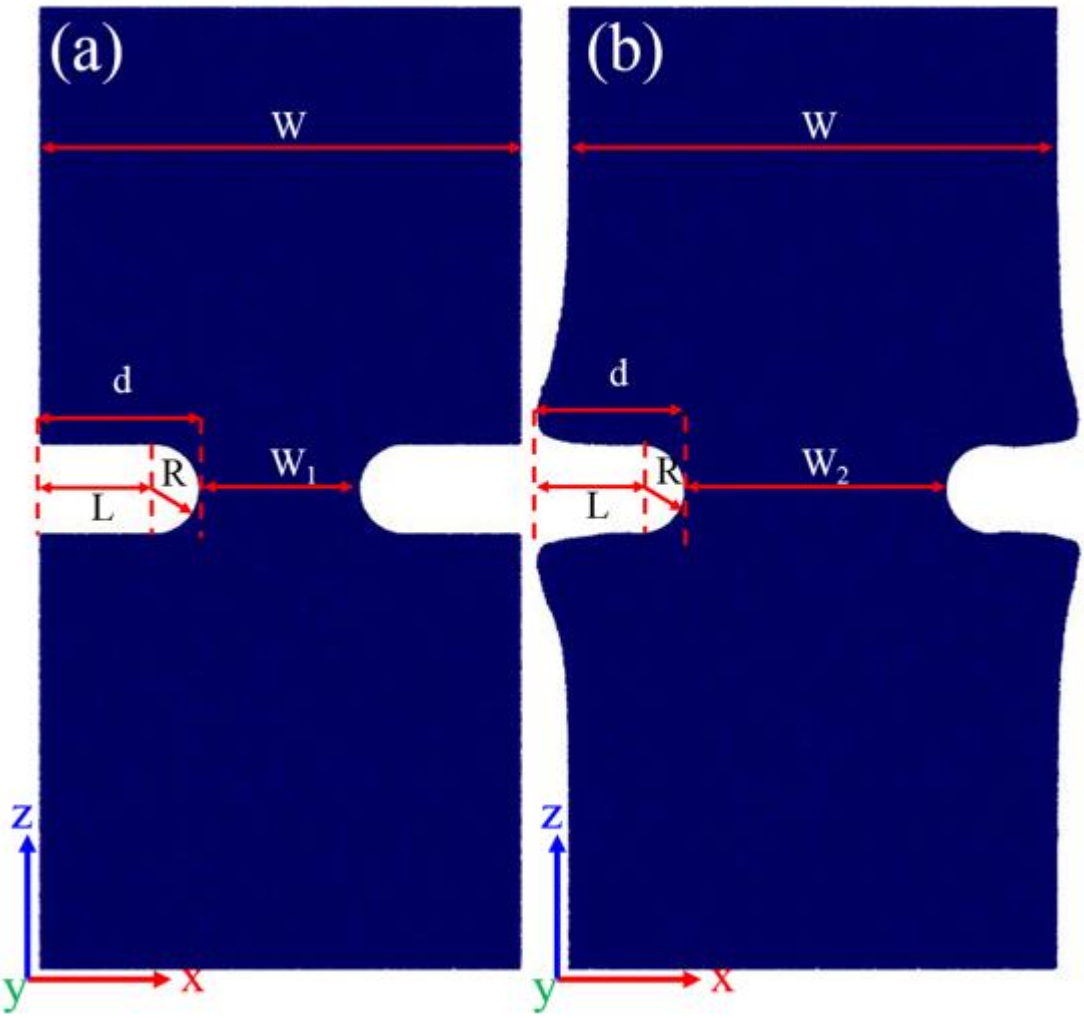

Figure 1. The schematic diagram of the notches formed by (a) cutting and (b) indenting respectively. L= 9 nm, R= 3.6 nm, d = 12.6 nm, W= 38.5 nm, W_1= 13.3 nm and W_2= 20.6 nm.

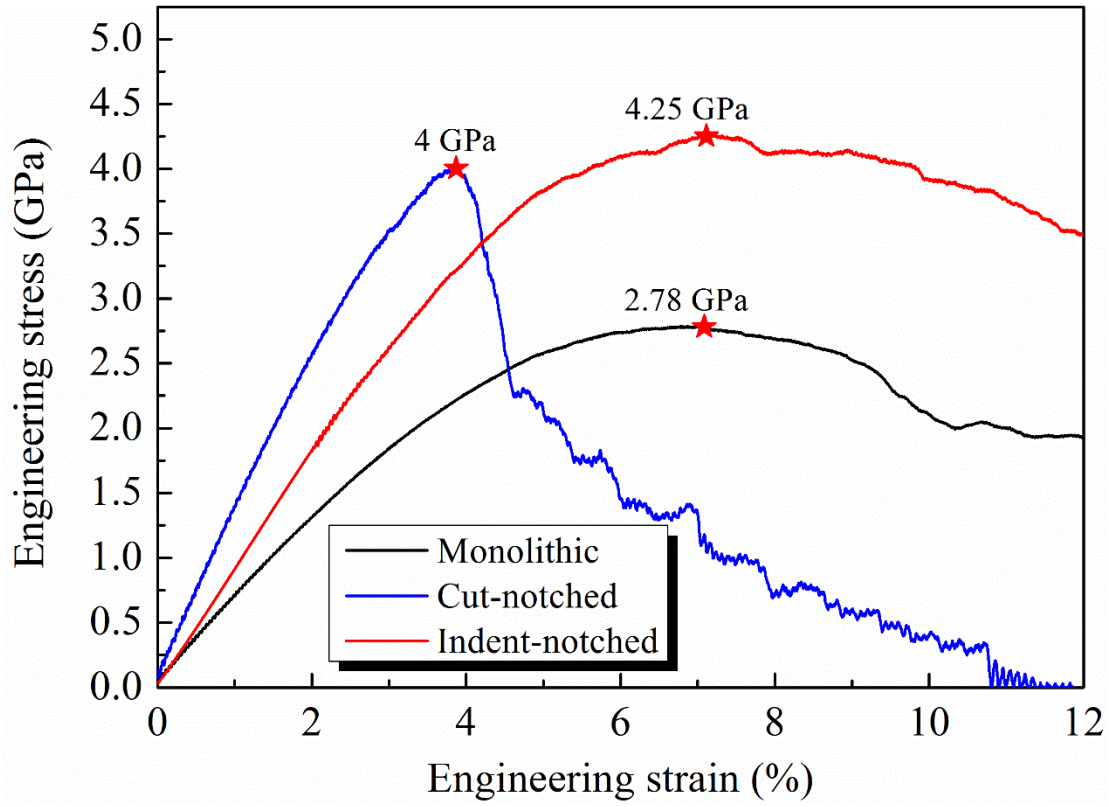

Figure 2. The engineering stress-strain curves of the monolithic, cut-notched and indent-notched $Zr_{36}Cu_{64}$ MGs.

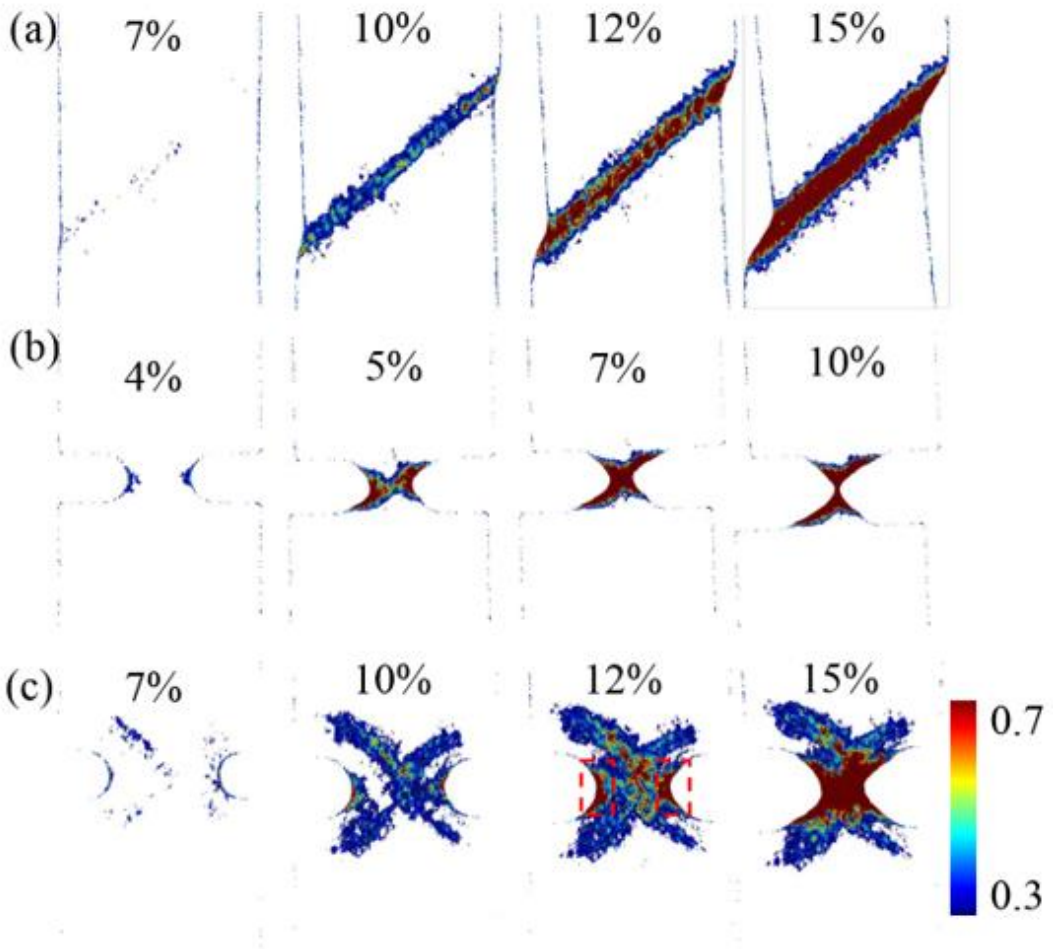

Figure 3. Snapshots of atoms with local shear strain greater than 0.3 at different strains for (a) the monolithic, (b) the cut-notched and (c) the indent-notched MGs.

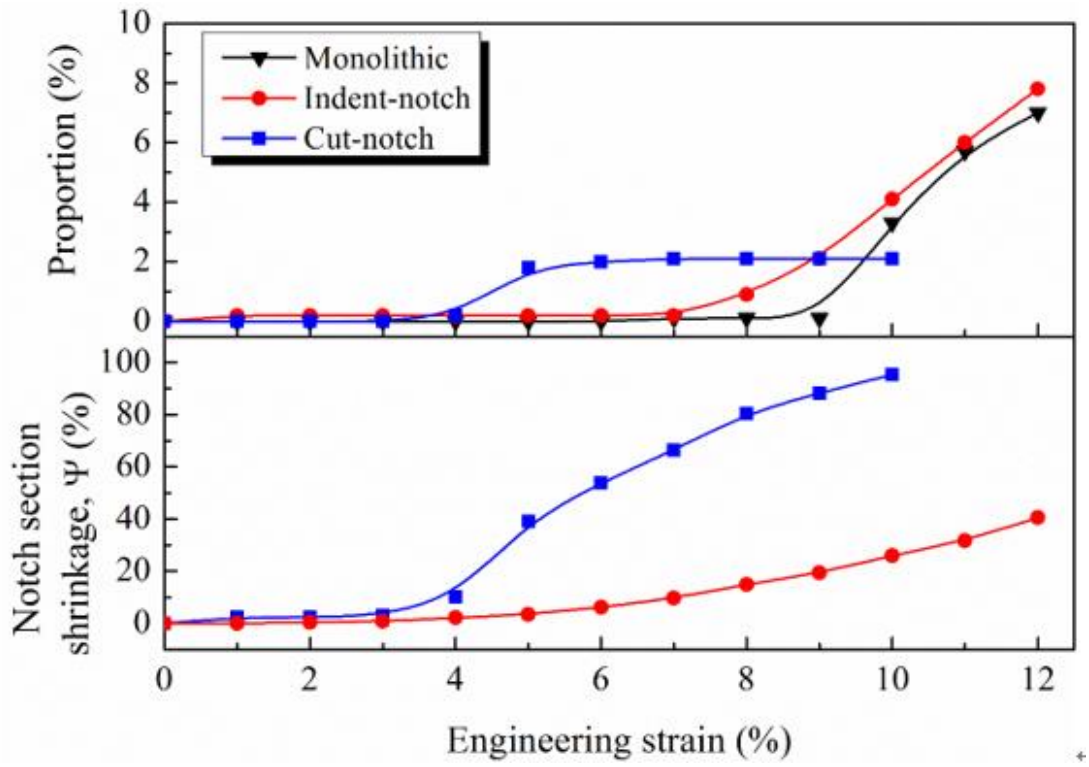

Figure 4. The proportions of atoms with local shear strain greater than 0.3 (upper panel) and the transverse shrinkage across the notch plane (down panel) for the MGs at different strains.

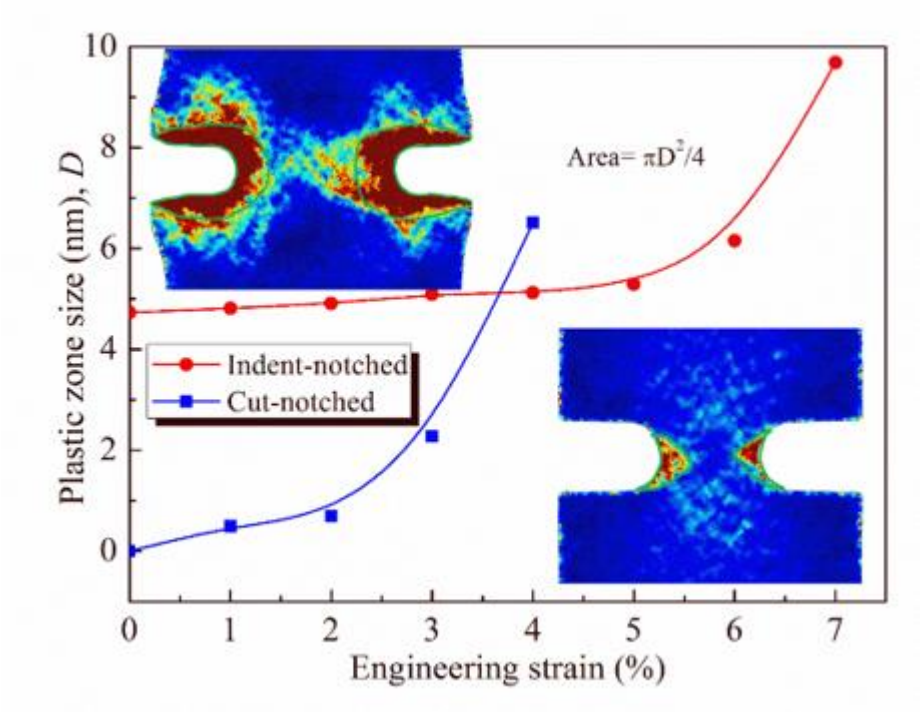

Figure 5. The plastic zone size (*D*) for the indent-notched and cut-notched MGs as a function of engineering strain. The inserted snapshot shows the plastic zone for the indent-notched and the cut-notched MGs.

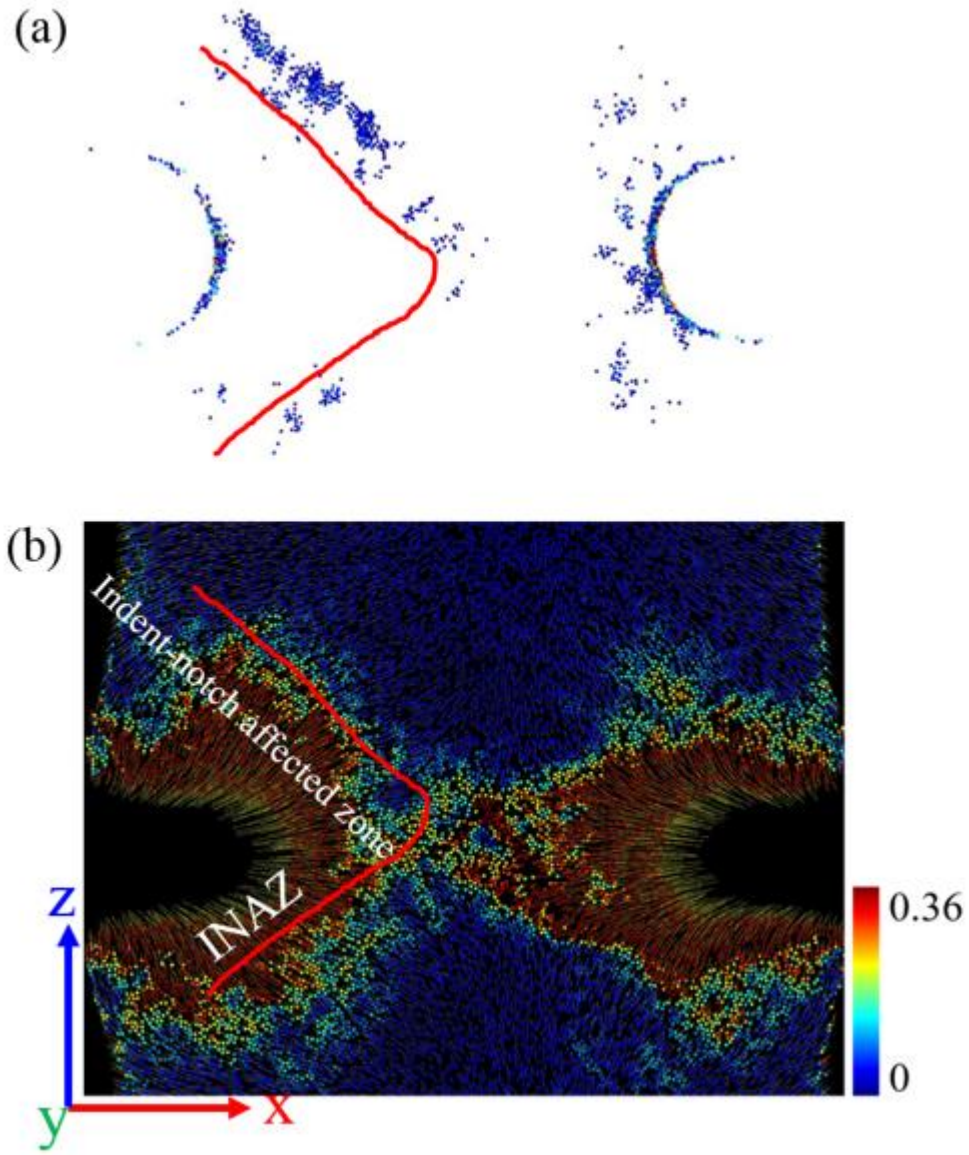

Figure 6. (a) The snapshot of atoms with local shear strain greater than 0.3 at a strain of 7% for the indent-notched MG, and the indent-notched MG at a strain of 0% is regarded as the reference state. (b) Atomic displacement vectors (yellow arrows) and local shear strain of the indent-notched MG at a strain of 0%, and the indent-notched MG before the indentation is regarded as the reference state. The red atomic region is called the indent-notch affected zone (INAZ).

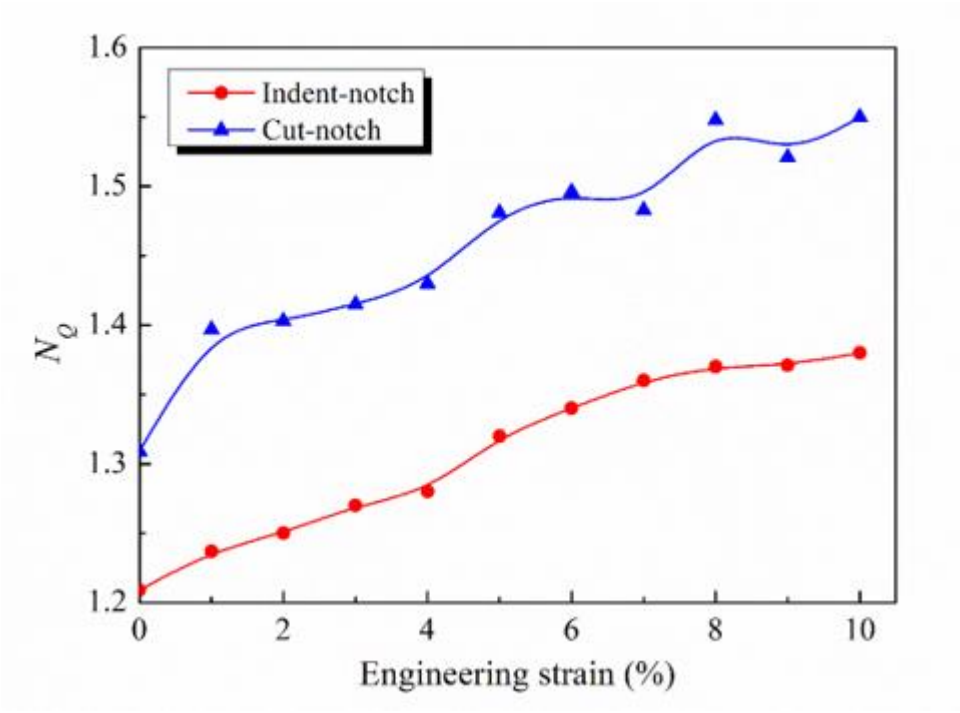

Figure 7. The average number of quasi-nearest atoms (N_Q) for the notched MGs at different strains.

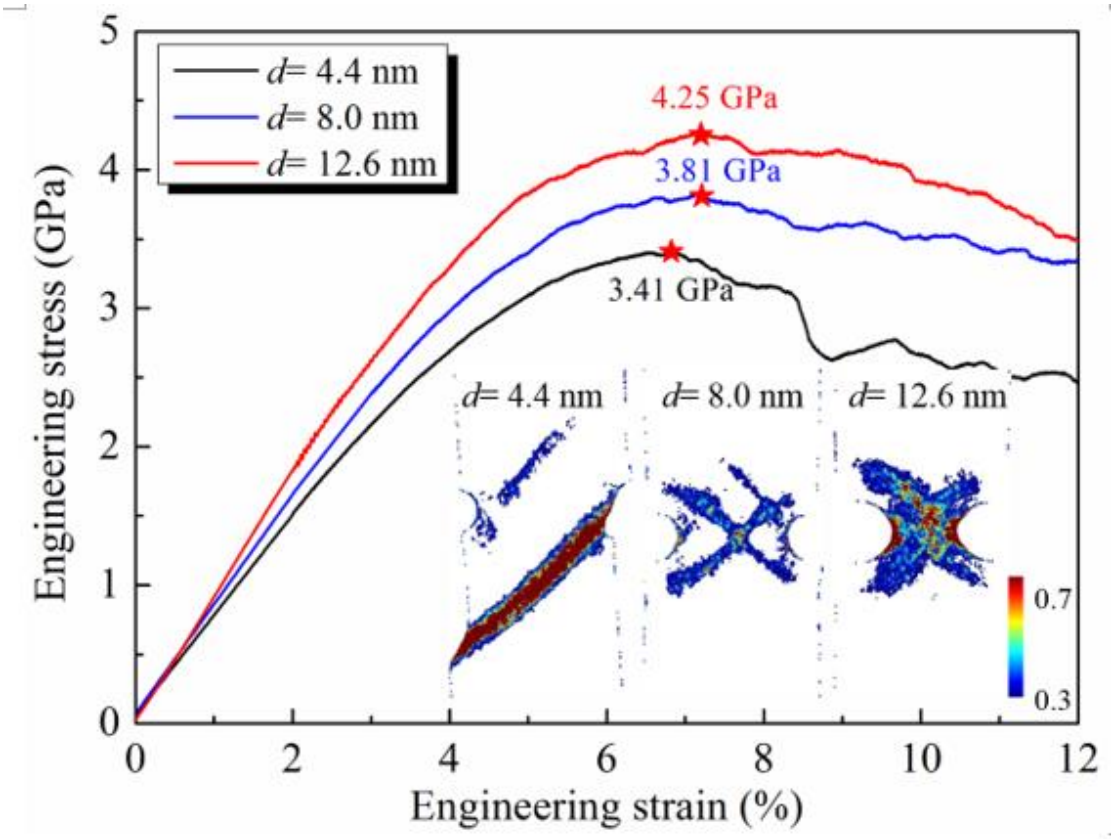

Figure 8. The engineering stress-strain curves of the indent-notched MGs with the notch depth equaling 4.4, 8.0 and 12.6 nm. The inserts show the snapshots of atoms with local shear strain greater than 0.3 at the strain of 12% for the indent-notched MGs with different notch depth.

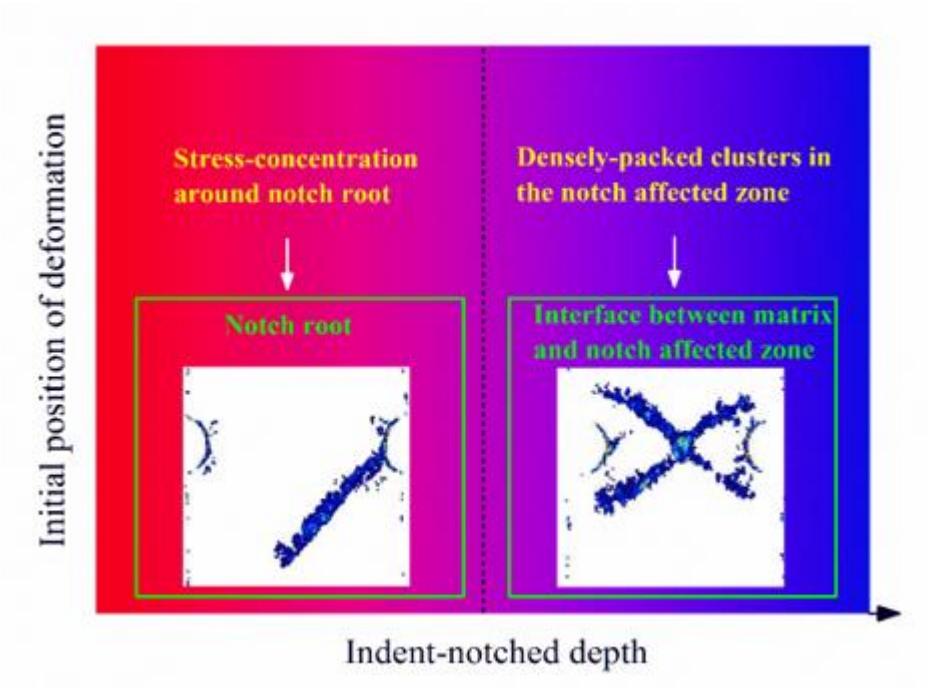

Figure 9. Schematic description of the competitive relationship between the densely-packed clusters composed of solid atoms in the NAZ and the stress-concentration around the notch root in the dominant role in the initial position of deformation accompanied by the notch depth.